Structure of Factor VII Gla domain bound to EPCR

Jacinto López-Sagaseta[1,2,3*], María Gilda Dichiara-Rodríguez[1,2.3]

[1]Unit of Protein Crystallography and Structural Immunology, Navarrabiomed, Navarra, Spain.
[2]Public University of Navarra (UPNA), Pamplona, Navarra, Spain.
[3]Navarra Hospital Complex (CHN), Pamplona, Navarra, Spain.

*To whom correspondence should be addressed: jacinto.lopez.sagaseta@navarra.es

Abstract

During the past few decades, numerous studies provided evidence for a productive interaction between activated factor VII (FVIIa) and the endothelial protein C receptor (EPCR). However, a structure that settles the docking orientation and binding signature was still lacking. We report here the crystal structure of factor VII Gla domain bound to human EPCR, revealing a binding geometry in essence indistinguishable from that of the PC-EPCR interface. FVII Gla locks onto EPCR's surface through the cooperative contribution of Ca^{2+} ions, residues of gamma carboxyglutamic acid and the hydrophobic ω-loop, essentially recapitulating PC docking, and confirming absolute structural competition for EPCR binding. These findings resolve a long-standing gap and inform the structural basis for the binding of a pharmacologically relevant coagulation factor to EPCR, illustrating the complete steric competition with PC. Such competition is dictated by a conserved Gla domain fold-driven mechanism of recognition with potential implications for pharmacological rFVIIa intervention in hemophilia.

Introduction

The endothelial cell protein C receptor (EPCR) is pivotal for normal mammalian homeostasis and development[1,2]. Tethered to the endothelial cell membrane, EPCR presents protein C (PC) zymogen to the thrombin-thrombomodulin complex, which in turn converts PC into the anticoagulant activated protein C (APC)[1]. EPCR-PC engagement is driven by the PC gamma-carboxyglutamic acid (Gla) domain, a structurally intricate region, where its conformation is the result of a fine-tuned interplay between residues of gamma-carboxyglutamic acid, Ca^{2+} and Mg^{2+} ions[3–5]. The binding blueprint is defined by a collection of well-defined H-bonds and non-polar contacts concentrated at one of EPCR's sides[3].

Over the past few decades, many groups have explored a potential interaction of EPCR with other Gla-containing factor, yet the debate gained clinical relevance with activated factor VII (FVIIa)[6–10]. This attention arose from the high circulating levels achieved upon administration of recombinant FVIIa (rFVIIa)[11], a current pharmacological intervention in the treatment of hemophilia. This scenario raised the question of whether the EPCR-FVIIa interaction could play an important role in the hemostatic potential of rFVIIa. *In vitro*, EPCR can inhibit tissue factor-dependent FVIIa coagulant activity[6]. *In vivo*, it was found that EPCR potentiates rFVIIa's hemostatic effect by competing with protein C[9].

Despite numerous studies have addressed the EPCR-FVIIa interaction, including mutational studies at the EPCR-FVII interface[6], a structure that confirms a coherent EPCR-FVIIa docking and provides the binding signature had not yet been reported and remained elusive. Here, we present the X-ray structure of FVII/FVIIa Gla domain bound to human EPCR, revealing the footprint of the interaction and a side-by-side comparison with that of the established EPCR-PC/APC interface.

Methods

Protein expression

The EPCR ectodomain (N30Q to reduce N-glycosylation) was cloned into the pcDNA3.4 secretion vector downstream an N-terminal TwinStrepTag® followed by a 3C protease site. EPCR was isolated from the cell culture supernatant upon transient-expression in CHO-S cells, with a Strep-Tactin affinity column followed by size-exclusion chromatography. Tag-free and deglycosylated EPCR was achieved by incubation with 3C protease and PNGase (produced in-house), with the enzymes being removed through a NiNTA resin prior to concentration and storage of EPCR target protein.

Crystallization of FVII Gla-EPCR complex

Pure, tag-free and deglycosylated EPCR was mixed with a 3-fold molar excess of FVII Gla peptide in the presence of $CaCl_2$ and $MgCl_2$. The protein-peptide complex was recovered via size-exclusion chromatography and concentrated prior to crystallization. Crystals of FVII Gla-EPCR complex were obtained by the sitting-drop vapor diffusion at room temperature and cryoprotected with glycerol before freezing.

Resolution of the FVII Gla-EPCR complex structure

X-ray diffraction data were collected at Xaira beamline. Diffraction spots were processed with XDS[12] and Aimless[13] packages. Structure solution was achieved via molecular replacement with Phaser[14], using EPCR (PDB 1L8J) and FVII Gla domain (1DAN) atomic coordinates as reference models. The structure was refined with Phenix.refine[15], with iterative manual building in Coot[16].

Results and discussion

The crystal structure of EPCR with bound FVII Gla domain was solved at 3.0 Å resolution, with four EPCR-FVII Gla complexes in the asymmetric unit (Figure 1 and Supplementary Table 1). Unambiguous electron density enabled the identification of the docking mode and the binding interface, including the ω-loop and Ca^{2+} ions that are part of FVII Gla domain. EPCR presents its canonical CD1-like fold, including the hydrophobic tunnel filled with a phospholipid (Figure 1A). The bound FVII Gla is located at one of receptor's ends, and contacts EPCR through H-bonds mediated by Gla7, Gla25 and Gla29, and indirectly, via Ca^{2+} coordination (EPCR Glu86 with Gla 7, 26 and 29). Essentially replicating PC docking

geometry (Figure 1B), FVII Gla ω-loop contributes with non-polar interactions, triggering a conformational change in EPCR Arg156, that releases space for accommodation of Phe4, tightly positioned adjacent to EPCR Gln75 and Tyr154 (Figure 1A and 1C). Leu5 and Leu8 are also located at a distance suitable for participating with hydrophobic and Van der Waals contacts. EPCR's hydrophobic groove houses a bound phospholipid[3,17–19], whose phosphate group, structurally exposed outwardly, attracts Arg156 side chain through electrostatic interactions (Figure 1A). Overall, the binding mode is indistinguishable from that previously observed for protein C Gla domain (Figure 1B). Likewise, a set of up to seven divalent cations, mainly Ca^{2+} ions, are distributed within FVII Gla residues, coordinating and driving a stable conformation that provides, ultimately, a productive binding to EPCR. The presence of Mg^{2+} ions had been previously reported to enhance the binding to EPCR[4,5], therefore, $MgCl_2$ was included in the crystallization conditions on purpose. We observed strong Fo-Fc electron density for five ion binding sites consistent with a scattering power for Ca^{2+} ions rather than Mg^{2+} (Figure 1D). Two additional sites with weaker Fo-Fc peaks were more ambiguous as they could represent Mg^{2+} with full occupancy, but also Ca^{2+} with partial occupancy (Figure 1D). These results agree with previous reports that demonstrated the binding of both types of ions to PC and FVII Gla[3,5,20].

Structural alignment of FVII Gla-EPCR and PC Gla-EPCR (PDB 1LQV) complexes with EPCR as reference frame reveals a highly accurate superposition (0.305 Å) of both Gla domains. The ω-loops in each Gla shows almost perfect overlap and orientation relative to EPCR, as well as near identical footprints on the receptor's surface (Figure 1E). The overall docking geometry presents a buried surface area of 468 $Å^2$ for the binding interface (Figure 1E), which, again, is similar with that observed in the PC Gla-EPCR complex (467 $Å^2$), suggesting that FVII Gla-EPCR interaction is solid and energetically coherent. An additional contact was observed between Gln85 and the backbone oxygen of Gla7 in the FVII Gla–EPCR complex. However, this interaction occurs at a distance of ~ 4 Å and is present in only one of the four complexes within the asymmetric unit; therefore, it is unlikely to represent a relevant interaction.

Prior alanine-scan mutagenesis[6] found a limited number of residues in EPCR critical for FVIIa binding, with many being equivalent to those identified structurally as key for the PC Gla-EPCR interaction[3]. This suggested that FVII/FVII Gla engagement on EPCR shared with PC a highly similar binding site on EPCR's surface. The FVII Gla-EPCR structure shows that Leu82, Glu86, and Arg87, all located in EPCR α1 helix, conform a cluster of direct contacts with the FVII Gla. Leu82 participates with hydrophobic packing interactions with FVII Gla7 and Leu8 backbone atoms, whereas Glu86 and Arg87 establish, respectively, H-bonds with Gla7 and Gla29 and salt bridges with Gla25 (Figure 2A). On EPCR α2 helix, Gln150 and Tyr154 establish direct H-bonds with Gla7 (Figure 2B), with Tyr154 also reported to be fundamental for binding of FVIIa[6]. Thus, these contacts further contribute to the overall strength of the FVII Gla-EPCR interaction. Additional contacts mediated by a coordinating Ca^{2+} ion were observed, which links Glu86 in EPCR with Gla26 in FVII Gla domain, and creates a more robust network of interactions with Gla7 and Gla29, in all cases, in a manner highly similar with that of the PC-EPCR interface (Figure 2C). Phe146 and Arg158, also

pivotal for FVII binding[6], contribute internally to a stable EPCR architecture. Phe146, close to EPCR Leu82 and Val83, plays a stabilizing role in a local hydrophobic site underneath FVII Gla binding surface, while Arg158's side chain engages Arg130 and Ala131 backbone atoms in an adjacent EPCR β-strand, thereby supporting the structural integrity of EPCR.

Like PC, the EPCR–FVIIa interface is also dominated by non-polar intermolecular contacts. Our structure reveals precise interactions between EPCR and the FVIIa Gla domain (Figure 3). Electron density supports docking of the Gla ω loop onto the EPCR surface adjacent to the bound lipid, with Phe4, Leu5, and Leu8 located at the core of the binding interface (Figure 3A). Surface comparisons show that FVII Gla occupies a similar EPCR binding pocket as protein C, adopting an analogous docking pose (Figure 1B). We also observed conserved hydrophobic and Van der Waals contacts at the binding interface. These involve Gln75 and Arg156 in EPCR and are mediated by the Gla ω loop Phe4 and Leu5 residues, as well as Leu8, beyond this loop (Figure 3C). A particular attention is deserved to Tyr154, which provides a dense set of non-polar interactions with the Gla N-terminal region (Figure 1D).

This structure provides definitive evidence for genuine FVII-EPCR interaction and addresses a long-lasting question pertaining EPCR restriction to PC/APC. Our crystal structure confirms that EPCR is not restricted to PC/APC, but instead, can be targeted by the Gla domain of FVII through a highly conserved docking mode. Pharmacological interventions with rFVIIa lead to a notable elevation in plasma levels, boosting the potential for EPCR to capture FVIIa instead of PC. In agreement with previous reports, this molecular competition would have an impact in the generation rate of APC, and, consequently, in the anticoagulant system.

References

1. Esmon CT. *The Protein C Pathway**. www.chestjournal.org

2. Li W, Zheng X, Gu JM, et al. Extraembryonic expression of EPCR is essential for embryonic viability. *Blood*. 2005;106(8):2716-2722. doi:10.1182/blood-2005-01-0406

3. Oganesyan V, Oganesyan N, Terzyan S, et al. The crystal structure of the endothelial protein C receptor and a bound phospholipid. *J Biol Chem*. 2002;277(28):24851-24854. doi:10.1074/jbc.C200163200

4. López-Sagaseta J, Montes R, Hermida J. Recombinant expression of biologically active murine soluble EPCR. *Protein Expr Purif*. 2009;64(2):194-197. doi:10.1016/j.pep.2008.11.002

5. Vadivel K, Agah S, Messer AS, et al. Structural and functional studies of γ-carboxyglutamic acid domains of factor VIIa and activated protein C: Role of magnesium at physiological calcium. *J Mol Biol*. 2013;425(11):1961-1981. doi:10.1016/j.jmb.2013.02.017

6. Lopez-Sagaseta J, Montes R, Puy C, Diez N, Fukudome K, Hermida J. Binding of factor VIIa to the endothelial cell protein C receptor reduces its coagulant activity. *J Thromb Haemost*. 2007;5(9):1817-1824. doi:10.1111/j.1538-7836.2007.02648.x

7. Preston RJ, Ajzner E, Razzari C, et al. Multifunctional specificity of the protein C/activated protein C Gla domain. *J Biol Chem*. 2006;281(39):28850-28857. doi:10.1074/jbc.M604966200

8. Ghosh S, Pendurthi UR, Steinoe A, Esmon CT, Rao L V. Endothelial cell protein C receptor acts as a cellular receptor for factor VIIa on endothelium. *J Biol Chem*. 2007;282(16):11849-11857. doi:10.1074/jbc.M609283200

9. Keshava S, Sundaram J, Rajulapati A, Esmon CT, Pendurthi UR, Vijaya Mohan Rao L. Factor VIIa interaction with EPCR modulates the hemostatic effect of rFVIIa in hemophilia therapy: Mode of its action. *Blood Adv*. 2017;1(15):1206-1214. doi:10.1182/bloodadvances.2016004143

10. Disse J, Petersen HH, Larsen KS, et al. The endothelial protein C receptor supports tissue factor ternary coagulation initiation complex signaling through protease-activated receptors. *J Biol Chem*. 2011;286(7):5756-5767. doi:10.1074/jbc.M110.201228

11. Roberts HR, Monroe DM, White GC. The use of recombinant factor VIIa in the treatment of bleeding disorders. *Blood.American Society of Hematology*. 2004;104(13):3858-3864. doi:10.1182/blood-2004-06-2223

12. Kabsch W. XDS. *Acta Crystallogr D Biol Crystallogr*. 2010;66(Pt 2):125-132. doi:10.1107/s0907444909047337

13. Evans PR, Murshudov GN. How good are my data and what is the resolution? *Acta Crystallogr D Biol Crystallogr*. 2013;69(Pt 7):1204-1214. doi:10.1107/S0907444913000061

14. McCoy AJ, Grosse-Kunstleve RW, Adams PD, Winn MD, Storoni LC, Read RJ. Phaser crystallographic software. *J Appl Crystallogr*. 2007;40(Pt 4):658-674. doi:10.1107/S0021889807021206

15. Adams PD, Afonine P V, Bunkoczi G, et al. PHENIX: a comprehensive Python-based system for macromolecular structure solution. *Acta Crystallogr D Biol Crystallogr*. 2010;66(Pt 2):213-221. doi:10.1107/s0907444909052925

16. Emsley P, Lohkamp B, Scott WG, Cowtan K. Features and development of Coot. *Acta Crystallogr D Biol Crystallogr*. 2010;66(Pt 4):486-501. doi:10.1107/s0907444910007493

17. Lopez-Sagaseta J, Puy C, Tamayo I, et al. sPLA2-V inhibits EPCR anticoagulant and antiapoptotic properties by accommodating lysophosphatidylcholine or PAF in the hydrophobic groove. *Blood*. 2012;119(12):2914-2921. doi:10.1182/blood-2011-05-353409

18. Erausquin E, Morán-Garrido M, Sáiz J, et al. Identification of a broad lipid repertoire associated to the endothelial cell protein C receptor (EPCR). *Sci Rep*. 2022;12(1). doi:10.1038/s41598-022-18844-y

19. Erausquin E, Rodríguez-Fernández A, Rodríguez-Lumbreras LÁ, Fernández-Recio J, Dichiara-Rodríguez MG, López-Sagaseta J. Structural vulnerability in EPCR suggests functional modulation. *Sci Rep*. 2024;14(1). doi:10.1038/s41598-024-53160-7

20. Lopez-Sagaseta J, Montes R, Hermida J. Recombinant expression of biologically active murine soluble EPCR. *Protein Expr Purif*. 2009;64(2):194-197. doi:10.1016/j.pep.2008.11.002

Data availability

Atomic coordinates and structure factors have been deposited and are available at the Protein Data Bank under the accession code PDB ID 9TJX.

Funding

This work was funded by the Ministry of Science, Innovation and Universities of Spain through the Ramon y Cajal program (GRANT RYC-2017-21683) and the State Program to Promote Scientific-Technical Research and its Transfer (GRANT PID2022-139888NB-I00).

Acknowledgements

We are grateful to the staff of Xaira beamline at ALBA Synchrotron for their assistance with X-ray diffraction data collection.

Autorship contributions

Conceived research: JLS; Performed experiments: JLS, GDR; Data collection and analysis: JLS; Draft writing: JLS.

Disclosure of Conflicts of Interest

The authors declare no competing interests.

Figure legends

Figure 1. Structural basis for FVII Gla domain binding to EPCR. (A) FVII Gla domain (light blue) is shown bound to EPCR (yellow), with coordinating Ca^{2+} and Mg^{2+} ions displayed as cyan and orange spheres, respectively. N-glycosylation at position Asn119 in EPCR is represented as sticks. The phospholipid molecule, also shown in sticks, is bound inside the groove formed by the two EPCR alpha helices. (B) Structural superposition of the FVII Gla–EPCR complex (blue) with that of the PC Gla-EPCR complex, PDB 1LQV (gray). (C) The FVII Gla domain–EPCR structure is displayed in combination with experimental electron density. The 2Fo–Fc electron density maps are contoured at 1.0 σ (blue mesh for FVII Gla, yellow for EPCR), illustrating the experimentally-determined docking and well-defined signal for both the FVII Gla domain and EPCR molecules at the binding interface. (D) Positive Fo-Fc electron density (green) determined by omitting the Ca^{2+} and Mg^{2+} ions (cyan and orange spheres, respectively) that contribute to FVII Gla overall fold and EPCR binding. (E) Two views of the residues in EPCR (shown as a grey surface) that directly participate in contacts with FVII Gla are indicated and highlighted in blue color. For reference, the footprint of PC Gla is also shown.

Figure 2. Comparison of Gla domain-EPCR polar contacts in PC and FVII complexes. (A) H-bonds bonds and salt bridges (black dashed lines) established between Glu86 and Arg87 in EPCR with several Gla residues in FVII and PC Gla domains, including Gla7, Gla9 and Gla25. (B) H-bonds mediated by Gla7 residues in PC (gray) and FVII (purple) complexes are indicated. All residues that participate in the interactions are indicated and highlighted as sticks.

(C) Additional Ca^{2+}-dependent contacts formed by Glu86 with Gla7 and Gla29 but also with Gla26. Ca^{2+} ions are shown in gray (PC complex) and blue color (FVII complex). The PC complex highlights also a water molecule (cyan) coordinated by the Ca^{2+} ion.

Figure 3. Conserved hydrophobic interactions are critical for FVII-EPCR binding. (A) Close-up view of the FVII Gla N-terminal ω loop bound to EPCR. The FVII Gla backbone is displayed as sticks in purple and EPCR as cartoon in yellow. The gray mesh indicates 2Fo–Fc electron density, while the green mesh represents positive Fo–Fc difference density, confirming the location of FVII ω loop Phe4 in between EPCR alpha helices. (B) Surface representation of EPCR in yellow color, with hydrophobic residues (Ala/Val/Leu/Ile/Met/Phe/Tyr/Trp) highlighted in gray. The PC and FVII Gla domains are shown in cartoon mode bound to EPCR with the same color configuration. Side-by-side comparison of Phe4, Leu5 and Leu8 residues of the PC and FVII ω loops, highlighted as sticks and occupying a hydrophobic pocket in EPCR upper region. (C) Non-polar contacts (dashed lines) established between EPCR and the Gla domains of PC (gray) and FVII (blue). (D) Tyr154 mediates a dense set of Van der Waals and hydrophobic interactions with the Gla domain N-terminal residues in both PC and FVII complexes, indicating the highly conserved binding mechanism.

Figure 1

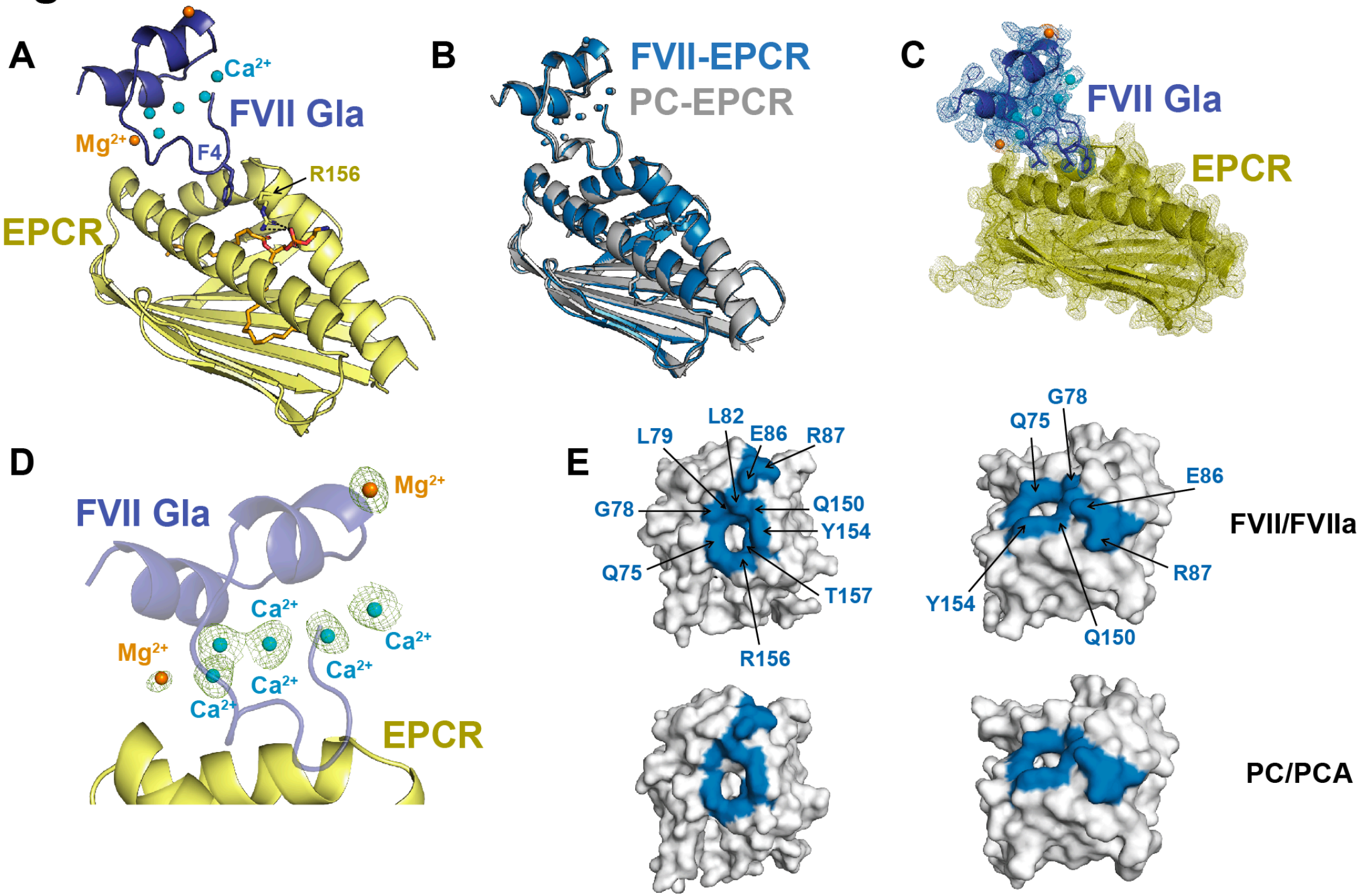
A
Ca2+
FVII Gla
Mg2+
F4
R156
EPCR
B
FVII-EPCR
PC-EPCR
C
FVII Gla
EPCR
D
FVII Gla
Mg2+
Ca2+
Mg2+
Ca2+
Ca2+
Ca2+
Ca2+
EPCR
E
L79
L82
E86
R87
G78
Q150
Y154
Q75
T157
R156
G78
Q75
E86
FVII/FVIIa
R87
Y154
Q150
PC/PCA

Figure 2

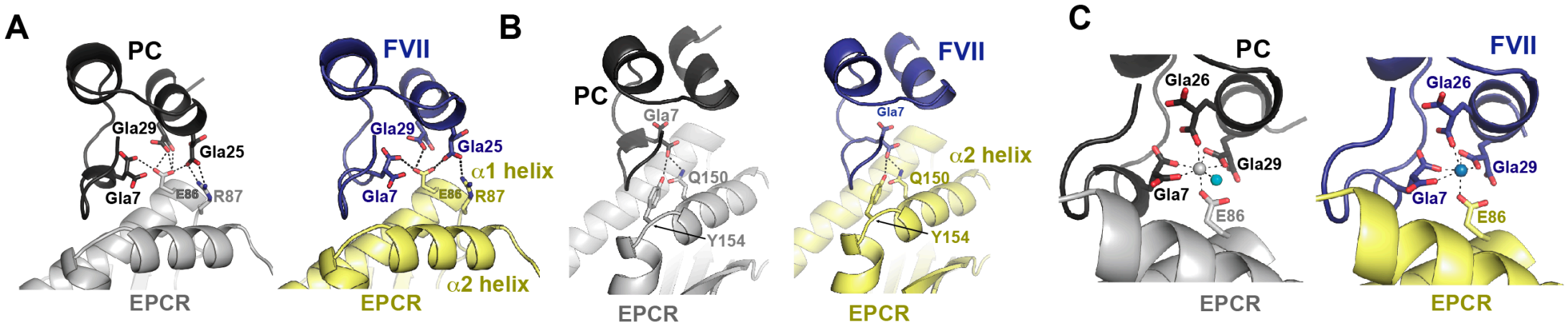
A
PC
Gla29
Gla25
Gla7
E86
R87
EPCR
FVII
Gla29
Gla25
α1 helix
Gla7
E86
R87
α2 helix
EPCR
B
PC
Gla7
Q150
Y154
EPCR
FVII
Gla7
α2 helix
Q150
Y154
EPCR
C
PC
Gla26
Gla29
Gla7
E86
EPCR
FVII
Gla26
Gla29
Gla7
E86
EPCR

Figure 3

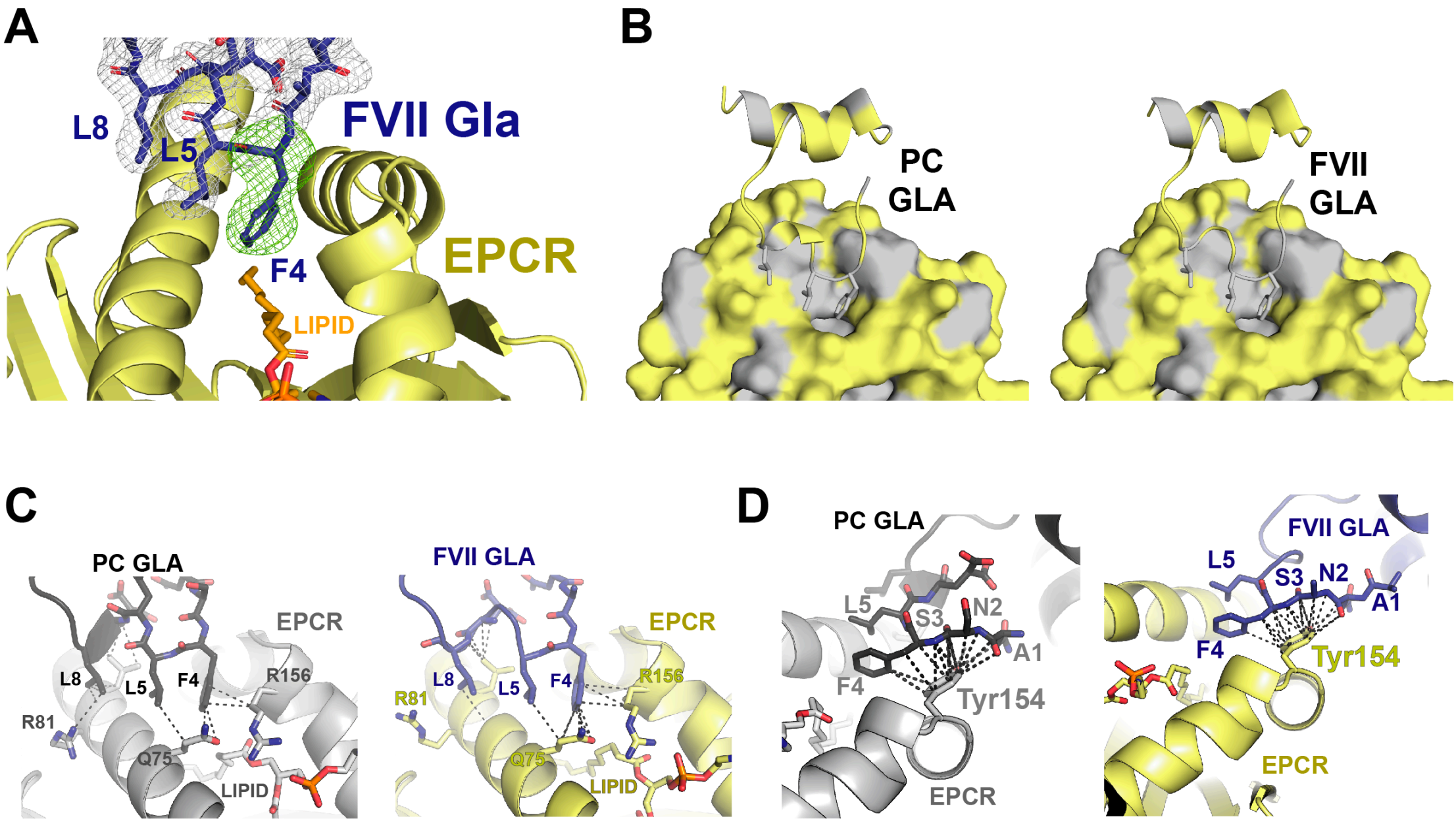
A
L8
L5
FVII Gla
EPCR
F4
LIPID
B
PC
GLA
FVII
GLA
C
PC GLA
EPCR
L8
L5
F4
R156
R81
Q75
LIPID
FVII GLA
EPCR
L8
L5
F4
R156
R81
Q75
LIPID
D
PC GLA
L5
S3
N2
A1
F4
Tyr154
EPCR
FVII GLA
L5
S3
N2
A1
F4
Tyr154
EPCR